

PROCEEDINGS OF SPIE

[SPIDigitalLibrary.org/conference-proceedings-of-spie](https://spiedigitallibrary.org/conference-proceedings-of-spie)

Substrates and mounting techniques for the High-Energy Focusing Telescope (HEFT)

Charles J. Hailey, Salim Abdali, Finn Erland Christensen,
William W. Craig, Todd R. Decker, et al.

Charles J. Hailey, Salim Abdali, Finn Erland Christensen, William W. Craig, Todd R. Decker, Fiona A. Harrison, Mario A. Jimenez-Garate, "Substrates and mounting techniques for the High-Energy Focusing Telescope (HEFT)," Proc. SPIE 3114, EUV, X-Ray, and Gamma-Ray Instrumentation for Astronomy VIII, (15 October 1997); doi: 10.1117/12.278902

SPIE.

Event: Optical Science, Engineering and Instrumentation '97, 1997, San Diego, CA, United States

Investigation of substrates and mounting techniques for the High Energy Focusing Telescope (HEFT)[†]

Charles J. Hailey^a, Salim Abdali^b, Finn E. Christensen^b, William W. Craig^a, Todd R. Decker^a, Fiona A. Harrison^c, Mario A. Jimenez-Garate^a,

^aColumbia Astrophysics Laboratory, Columbia University
538 West 120th Street New York, NY 10027

^bDanish Space Research Institute, Juliane Maries Vej 30, DK-2100
Copenhagen, Denmark

^cSpace Radiation Laboratory, California Institute of Technology
MC 220-47, Pasadena, CA 91125

ABSTRACT

The High Energy Focusing Telescope (*HEFT*) is a balloon-borne system for obtaining arcminute imagery in the 20-100 keV energy band. The hard X-ray optics are baselined to use thin epoxy-replicated aluminum foil substrates coated with graded-d multilayers, and we show some results on X-ray performance of prototype foil substrates. We also propose an extremely promising alternative substrate - thermally-formed glass. The advantages of thermally-formed glass substrates, their fabrication and preliminary metrology on sample pieces are discussed. If ultimately feasible, the thermally-formed glass is a better substrate due to its superior hard X-ray reflectivity and scattering properties in comparison to similarly coated epoxy-replicated aluminum foil. We also discuss some preliminary work on the *HEFT* mirror mounting concept and the associated angular resolution error budget.

Keywords: X-ray optics, multilayers, thin foil optics

1. INTRODUCTION

Hard X-ray astronomy (20-100 keV) has been handicapped with respect to sub-10 keV X-ray astronomy primarily because of the lack of true imaging capability. The problem for hard X-ray astronomy is not merely an inability to obtain high resolution images. Rotation modulation collimators (RMCs) have been used to obtain arcsecond resolution images of the sun in hard X-rays¹. Recently the *GRATIS* balloon payload obtained arcminute resolution imagery of cosmic sources in the 20-150 keV energy band using the rotated coded aperture technique². The difficulty with pseudo-imaging techniques such as coded apertures and RMCs is that they produce images without concentrating the source radiation in pixels distinct from the background radiation. This failure to concentrate the source photons means that pseudo-imagers do not suppress the diffuse background in proportion to the number of pixels in the detector, as true imaging optics do. Consequently the sensitivity of the pseudo-imagers employed in hard X-ray astronomy is greatly reduced compared to that of the grazing incidence, focusing optics employed at lower energies.

The prospects for employing grazing incidence optics in hard X-ray astronomy have drastically improved in the last few years. There has been rapid progress in the development of appropriate coatings for hard X-ray optics which enhance the reflectivity at the requisite small graze angles and over a broad energy band³.

[†] Correspondence: C.J. Hailey. chuckh@astro.columbia.edu; Telephone: (212) 854-4238; Fax: (212) 854 4648

These graded-d multilayer coatings, which utilize alternating layers of high and low atomic number materials (such as Ni/C or W/Si) provide coherent increases in reflectivity just like a natural crystal. But their d-spacing changes continuously with depth into the multilayer, so that a broad range of energies can be diffracted/reflected. The multilayers and their coating technologies place special demands on the substrate technology and the overall optics design.

2. THE HIGH ENERGY FOCUSING TELESCOPE

We are currently developing the High Energy Focusing Telescope (*HEFT*), a hard X-ray telescope for use on a balloon platform. A baseline description of the instrument characteristics is given in Table 1.

Instrument Characteristics	Value
Energy range	20-120 keV
Angular Resolution	1 arcminute
Field of view	17 arcminutes
Sensitivity (photons $\text{cm}^{-2} \text{s}^{-1} \text{keV}^{-1} 3\sigma$)	2×10^{-7} @ 40 keV
Line Sensitivity (photons $\text{cm}^{-2} \text{s}^{-1} 3\sigma$)	4×10^{-6} @ 68 keV
Energy resolution (FWHM)	900 eV @ 78 keV
Effective area	300 cm^2 @ 40 keV
Aspect reconstruction (rms)	6 arcseconds
Pointing stability (rms)	20 arcseconds
Time resolution	1 msec
Number of modules	14
Focal length	6 meter
Optics	Conical approximation Wolter 1

TABLE 1: Performance characteristics for *HEFT*.

The telescope consists of 14 modules of highly nested mirror shells in a conical approximation to the Wolter geometry. The mirror shells have an upper and lower section and each section is divided into quadrants for a total of 8 shell substrates per shell. Cadmium Zinc Telluride pixelated detectors are used to image the photons. Table 2 indicates some of the baseline parameters of the imaging optics to achieve the requisite goals.

Optics parameters	Value
Shell substrate	Epoxy replicated aluminum foil or thermally formed glass
Number of shells per module	72
Number of substrates per shell	8
Total number of substrates required	8064
Shell thickness	300 - 500 μm
Length/diameter ratio (outer shell)	2
Inner shell radius	4 cm
Outer shell radius	12 cm
Graze angle (outer shell)	17 arcminutes

TABLE 2: Optics design of *HEFT*

The baseline *HEFT* design utilizes epoxy-replicated aluminum foils (ERAFs). The gold-coated ERAFs are then overcoated with a graded-d multilayer to produce the final hard X-ray optic. In this paper we describe some results on X-ray performance of prototype ERAFs. We also describe some results on an exciting new

substrate technology for hard X-ray optics - thermally-formed glass. The substantial advantages of thermally-formed glass compared to ERAFs for hard X-ray optics are discussed. We also describe the basic concept for mounting the mirror shells, which will permit *HEFT* to obtain arcminute resolution imagery at low cost.

3. SUBSTRATE SELECTION

The enormous number of shells required for hard X-ray telescopes demand a substrate which can be easily fabricated in large numbers. Simple engineering constraints on the weight and available area on any realistic balloon or satellite platform require substrates of reasonably high strength to weight ratio and thickness ~ 0.2 - 0.5 mm. The substrate material must also hold its figure to the subarcminute level when used with the typical, conservative shell aspect ratios of 2-4, which have been commonly employed in space-qualified, X-ray grazing-incidence optics. The substrate material must maintain its figure in the non-benign mechanical and thermal environment of a balloon flight. On a satellite the substrate must additionally have long-term thermal stability. We have been working with epoxy-replicated aluminum foils as the baseline. As part of the *HEFT* project we are also investigating alternative substrates that would offer advantages over the epoxy-replicated foils. We discuss the various options here.

3.1 Epoxy replicated aluminum foil substrates

For moderate resolution (\sim few arcminute) and moderate cost X-ray optics an ideal substrate is aluminum. The aluminum can either be rolled to the appropriate figure (eg. *SODART*)⁵ or stress-relieved on a mandrel to obtain the figure (eg. *ASCA*)⁴. On *SODART* and *ASCA* the shorter wave ($< \sim$ few 100 micron) ripple was removed using the lacquer polishing technique first used on X-ray optics by Catura et al.⁶. The thin gold reflecting surface is deposited onto the lacquer-coated mirror. To obtain superior performance on Astro-E, through suppression of longer wave surface deformations, epoxy-replicated aluminum foils are being used⁴. Similar techniques were used to make X-ray mirrors on *EXOSAT* and some *XMM* prototype mirrors. The rolled aluminum foils are pressed onto a gold-coated mandrel, with a thin layer of epoxy to smooth out the surface ripple in the foils and mandrel. Using this technique very good X-ray reflecting surfaces with low X-ray scatter can be obtained. Together with simple to fabricate conical optics the ERAFs are a means to produce optics where large area is required at low cost.

The ERAF/conical mirror approach can be extended into the hard X-ray band. In this case, the gold-coated ERAF can be overcoated with the appropriate graded-d multilayer (typically Ni/C or W/Si). Epoxy replicated foils are the baseline optics for *HEFT*. We have a program in place to produce ERAFs for potential use as *HEFT* optics. Our procedure is straightforward. We first deposit gold on a glass substrate, using either DURAN or a glass with similar surface qualities ($\sigma \sim 4$ - 5 Å). This gold is then replicated onto an aluminum foil of 0.4mm thickness (the same raw material as that used on *SODART*) using Epon 828 epoxy. The Epon 828 was selected because an analysis of the stresses in the thin substrates indicated that the very low shrinkage of this epoxy both during and after cure would provide the best relief from shell figure distortions. The Epon 828 is also a relatively low out-gassing epoxy. The mixture is adjusted to produce a 35 μ m thick epoxy layer. X-ray scattering measurements, as shown in Figure 1, indicate a surface roughness of 4Å.

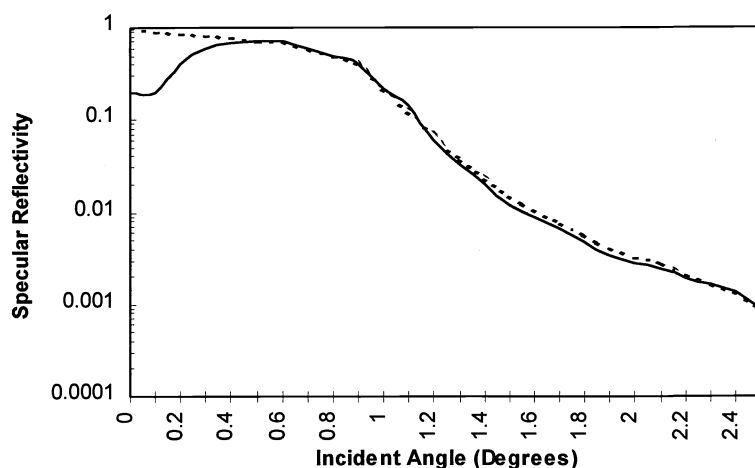


FIGURE 1: Specular reflectivity of an ERAF produced using the technique described in the text (solid line). The reference curve (dashed line), shows the ERAF surface roughness is consistent with a gold surface with a σ of 4 Å.

3.2 Glass substrates

The ERAFs offer performance consistent with the goals of *HEFT* described above. Nevertheless we are motivated to investigate alternate substrate technologies to see if even better hard X-ray performance can be obtained, and to see if the production process can be simplified. We have performed an extensive survey of thermally formed glass substrates as an alternative to ERAFs. Thermally-formed glass has many desirable properties. Glass provides a superior substrate for depositing multilayers. It is possible to obtain much better reflectivity and scattering performance on multilayer-coated glass than on ERAFs (see companion paper by Mao et al.). Moreover the glass shell production is a two step process involving a simple thermal forming procedure (see below) to obtain shell figure and an overcoating with the multilayer. Many shaped-shells can be formed per day. The reduction in production steps compared to ERAF fabrication would permit us to greatly accelerate the fabrication phase of *HEFT* and obtain higher sensitivity than anticipated in our baseline design, all at lower cost.

Glass is a natural choice as a substrate material for X-ray optics for other reasons. It has favorable mechanical properties, it can be produced with a very smooth surface, it can be made very flat over large areas and it can be produced in very thin uniform sheets. In the past, it was difficult to find a glass which possessed all of these favorable characteristics. The emergence of glass as the substrate of choice in flat panel displays has led to the development of several glass products which are ideal for producing X-ray optics. The glasses, known generically as ‘microsheet’, are used as the substrate on which active elements of flat panel displays are deposited. They must be extremely smooth on all length scales up to the size of the displays (~30cm), and must have good mechanical properties. We have studied a number of these glasses and selected two, Schott and Desag AF-45 and D-263 as potential candidates for forming substrates for our hard X-ray optics. These glasses are produced by a method, known as ‘overflow’, in which the glass sheet is never in mechanical contact with any surface. Deviations from uniformity are small, with the most pronounced error being a variation in thickness of 25 μm from one side of the sheet to the other. There are no measurable ripples or other small scale deviation.

A number of trial mandrels and forming procedures were attempted on this microsheet before satisfactory results were obtained. The test sample material thickness ranged from 300-400 μm . Variation in the thickness of the sheets was $\pm 25 \mu\text{m}$. The samples ranged in length from 10 to 20cm.

A stainless steel mandrel, a cylinder of 20 cm in length and a 7.5 cm diameter was used initially. The glass was placed over the mandrel, which had a surface finish generated from fine passes with a lathe, i.e. 'shiny' but not polished. The temperature was raised to 550C over a period of 2 hours, once stable, the temperature was maintained at this constant value for 1 hour. The oven was turned off and the sample/mandrel allowed to cool overnight. In this initial test, the sample adhered to the mandrel quite strongly and no usable pieces were produced. Assuming that the relatively crude surface finish was causing the adhesion we then finely polished the steel mandrel with the final polishing step being a 0.3 μm grit polishing cloth. The same heating and cooling procedure was used, and the sample still adhered to the mandrel, although it appears that the adhesion was less uniform than previously. We then repeated the procedure, after the mandrel had been polished again, with the addition of a graphite aerosol release agent. This trial produced a sample which separated cleanly from the mandrel after the cool down. The surface quality of the samples produced in these trials was uniformly poor. Waviness and dimples were apparent on length scales of a few millimeters. No quantitative measurements were done on the surface quality on either micro or mid-range scales. In an attempt to track down the source of these distortions, which were attributed to non-uniform adhesion on the surface, we made a number of changes to the procedure. The surface of the mandrel was clearly discolored after the thermal cycle, probably due to oxidation. The slumping procedure was repeated with a nitrogen purge of the glass oven. Although the mandrel appearance was better, the distortions on the glass surface were qualitatively unchanged. Because we used a solid steel mandrel, the cool down time was quite long and sample turnaround was slow. Each trial was done in the afternoon and the samples allowed to cool overnight.

The next mandrel material tried was a 7.5cm diameter quartz tube. Wall thickness was approximately 3mm and the mandrel was $\sim 20\text{cm}$ in length. The surface of the mandrel was prepared using a Graphite aerosol releasing agent and was then polished to leave a thin, uniform, film. The sample and mandrel were then raised to 550C over a 2 hour period and allowed to 'soak' at that temperature for 1 hour. Cool down process was much quicker than with the steel mandrel, typically about 2 hours. This faster cool down may have contributed to rather regular cracking of these samples during the cooling process. The glasses had different coefficients of thermal expansion and there was some residual adhesion between the glass sample and the mandrel. Experimentation with different thermal profiles and applications of the release agent did not produce a method which would consistently produce unbroken pieces. The larger pieces of the sample, however, showed a very encouraging surface quality. The surfaces were quite smooth and no distortions were evident. It appeared likely that this mandrel could be made to work with a proper release agent (or if one was willing to accept a rather low yield).

The next set of trials was done with the same size quartz tube, this time cut in half along its length producing a semi-cylindrical cavity into which the glass was slumped. The inside of the mandrel was again sprayed with a graphite release agent and polished. The glass was slumped into the tube over a range of temperatures (starting at the nominal 550C) and times. Initial results showed that this process worked well, there was no adhesion to the mandrel and the surface quality looked quite good visually (see atomic force microscope (AFM) results below). Experimenting with rise times and 'soak' times followed and we determined that the plateau temperature worked for a range from 500-525C. Rise times were decreased to 1 hour and 'soak' times to 35 minutes with no apparent degradation in results. The conformance to the figure of the mandrel appears to be very good, no visible gap was noted between the mandrel and the sample. There were occasional point defects on the sample surfaces. These were attributed to dust contamination on the surface. The slumping was done with no special attempts made to keep samples clean.

As these samples were the first to look promising we did a series of measurements to determine the μm scale roughness. A Park Scientific AFM was used to measure the roughness both before and after the

slumping. Square regions ranging in size from 1.2 to 5 μm on a side were measured. The flat sample, and then the inside and outside surface of the slumped piece were measured.

Surface Roughness (\AA)	X(rms)	X(avg)	Y(rms)	Y(avg)
Flat Sample	1.9-2.4	1.6-2.1	2.2-3.1	1.8-2.5
Slumped sample (inside)	3.5-5.7	2.0-2.7	9.0 - 12	7-8.5
Slumped sample (outside)	3.0-4.4	2.3-3.0	10.0-14	9.0-11

TABLE 3: AFM measurements on thermally formed glass samples.

The X direction is the 'long' direction, i.e. the optical axis. The Y axis is the direction that the glass was bent in. There has clearly been some degradation in the surface quality, although it is still acceptable along the optical axis (with the small FOV of these optics, off-axis rays are not a concern, only the 'X' direction is important). The degradation, in the form of ridges, occurs in a uniform fashion across the surface after slumping. The degradation in the X-ray performance of optics produced in this way would be minor.

Investigation of the source of this degradation and some unacceptable larger scale figure errors resulted in some final changes in the forming procedure that involved a redesign of the mandrel to reduce its thermal mass. In addition a separation layer was added between the mandrel and the glass surface. Ramp rates, soak times and set points were also adjusted to optimize the millimeter scale figure distortions in the piece. The forming procedure now produces substrates with acceptable roughness and large scale figure.

3.3 Figure measurements

The procedure for producing samples of appropriate figure for the *HEFT* optics has been perfected only recently. As the samples have increased in quality, the defects are smaller, in most cases, than our ability to measure them. New measurement facilities are under construction to allow a more complete characterization of the thermally formed glass. We report here on the results of preliminary figure and roughness measurements using existing facilities.

Length scale	Measurements	Value
few \AA to 5 μm	AFM	< 3 \AA
9 μm -- 550 μm	X-ray	5.9 \AA RMS
1mm-10mm	Optical	< 1.7 arcminute
10mm-300mm	Mechanical	< 2 arcminute

TABLE 4: Results of figure measurements on thermally formed glass samples.

3.3.1 X-ray measurements

X-ray measurements were done at DSRI on a thermally formed piece (gold coated at DSRI) using the Total Integrated Scattering (TIS) method in which the specular reflectivity is subtracted from the spectrum. For an incident angle of 0.4 degrees the derived σ was 5.9 \AA . The length scales sampled ranged from d_{min} of 9.4 μm to a d_{max} of 550 μm . This result is comparable to the roughness measured separately for the glass substrate itself, as expected.

3.3.1 Optical measurements

A laser scan of the surface of the thermally formed glass optics was used to investigate variations at the length scales of the laser beam spot size and larger. A laser beam, with spot size 1mm, was reflected off the surface of a thermally formed piece mounted to a precision translation stage. The line focus, as projected on a detector plane 8 meters away, was measured as the beam was scanned over the surface, in the direction of the optical axis, in 10 μm steps. The system is first calibrated by scanning a large optical flat. The uncoated thermally formed sample is then inserted directly on top of the optical flat. Then as the translation stage scans the beam across the sample a continual fiducial spot from the underlying flat

provides a real time check on the system. Distortions in the glass on scales comparable to the size of the probe beam can be seen as variations in the width or uniformity of the line focus as sampled 8 meters away. Variations in the position of the line focus indicate larger scale figure error. The current setup is systematic limited at about 1.5 arcminutes. A more precise setup is under construction. Typical results are given in Table 4.

3.3.1 Mechanical figure measurements

The optical system is useful for probing smaller scale figure. Larger scale figure, and the conformance of the thermally formed glass to its mandrel (which is not reflective), requires direct mechanical measurement. For these measurements the mandrel is mounted on a precision 3 axis translation stage. A dial indicator, set for low contact pressure, is used with a rounded tip to scan the entire surface of the piece. The sampling frequency is on order a few mm, adequate in this case as the predominant figure errors have length scale on order the sample size. The repeatability of the measurement is better than 1 arcminute (over the length scale of the piece) and is limited by the accuracy of the probe. The mandrel and thermally formed glass substrates are both measured with a mechanical probe. The force induced by the mechanical probe limits the accuracy of the measurement of the glass to ~ 2 arcminutes. The mechanical measurements show that the glass does conform to the mandrel at the 2 arcminute level. More precise measurements are underway.

3.4 Mechanical properties

Glass is an intrinsically strong material, in the thickness we propose it is more than strong enough to maintain figure under the loading expected during balloon launches or landings. However, it is brittle, and the practical strength of glass is always limited by flaws and cracks that serve as fracture points. We have a great deal of experience working with a similarly brittle material, SiC, which has been used successfully as the substrate material for the thin (1 mm) gratings on the *XMM* RGA⁹. We are applying the techniques developed there to ensure the glass substrates can be used under both balloon and satellite loads.

The first problem is limiting the size of flaws. The strength of glass decays exponentially with the size of the flaws in the material¹⁰. We have developed an edge cutting technique that limits edge flaws to length scales on order a few μm . This provides a practical tensile strength of ≥ 100 MPa which allows us to use techniques similar to that used on the *XMM* RGA to mount the glass pieces. The second problem is to reduce the point stresses caused by the mounting fixtures. Several techniques for mounting are under investigation, the most promising of these uses a visco-elastic material of precisely controlled thickness to coat the glass. This layer, which may either be used only at the point contacts, or over the entire 'back' side of the glass piece, distributes the load from the mounting points, eliminates induced cracks and curtails fracture growth. A representative fixture, containing several shells mounted in this fashion, is under construction. The shells will be mounted and shake tests performed to validate the concept.

4. OPTICS ERROR BUDGET AND ASSEMBLY/MOUNTING

Preliminary work has been completed on a design concept for assembly and mounting of the *HEFT* optics. It is compatible with either the ERAFs or thermally formed glass substrates. Because *HEFT* is a cost-constrained project, the main challenge is to develop a shell mounting scheme in which the structure utilizes only commercial machining tolerances on the optics bench yet permits *HEFT* to obtain subarcminute performance. We have adapted the mirror mounting scheme successfully employed on SODART¹¹, with some substantial modifications. Like SODART, radial spokes are used, with short grooves, similar to teeth on a comb, to index the shell perimeter into position against the back of the groove (Figure 2).

These spokes are located above the front shells, just below them, and below the rear shells. However, in distinction to SODART, where the radial spokes are free to move in order to adjust the shells, on *HEFT* the spoke positions will be fixed with a set of precision-placed pins. The spokes are stacked and the grooves machined simultaneously using an EDM process. This combination of pinning the spokes and machining

the grooves in the spokes simultaneously substantially reduces the placement errors associated with the grooves. The true positions of the shell substrates, and therefore the shell to shell variation in the radial direction, can be limited to $\leq 10 \mu\text{m}$. This turns out to be adequate, given an analysis of the principle errors

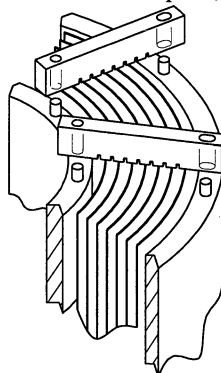


FIGURE 2: The mounting scheme concept for *HEFT* shells

in the optics system, to meet the *HEFT* goals. The primary error is associated with a variation in groove depth leading to a rotation of individual substrates (see below).

Given a baseline mounting concept with known machining tolerances, a preliminary error budget could be generated for the telescope half-energy width. Errors are divided into the following categories (Table 5)

- 1) Assembly errors: These include tilts and translations of front and rear shells/substrates together or separately and sizing (radius) errors,
- 2) Figure errors: This include taper errors and in and out of phase roundness errors due to the mounting scheme as well as intrinsic figure errors in the piece (eg. multilayer stress-induced distortions),
- 3) Conical error due to approximation of the confocal hyperbola-parabola of the Wolter Type I by a pair of semiconical segments
- 4) Hard X-ray scattering due to short wavelength, uncorrelated surface roughness.

Among these terms the assembly errors and the figure errors dominate the error budget. Hard X-ray scattering is fairly low (see companion paper by Mao et al.). The conical error is suppressed due to the long focal length of *HEFT*. The dominant assembly error is found to be due to rotations of the mirror substrates around the radial direction, which are allowed due to the use of commercial machining tolerances on the groove depth. This error could easily be reduced to negligible level through tighter machine tolerances but this would drive up the cost unacceptably for a balloon-project, although it would be entirely feasible for a satellite project. The tolerancing is sufficiently tight so that out of phase roundness errors are negligible and in phase roundness errors are suppressed because of the long focal length (since this error is proportional to $1/F$). The dominant contributions to the figure error are intermediate scale roughness and large scale figure errors. The mounting scheme effectively removes the latter, except for some residual small effect expected due to multilayer stresses. The large scale figure error in unconstrained pieces was determined by a separate analysis of bimaterial bending due to epoxy shrinkage, temperature effects and multilayer stresses in the ERAFs or glass pieces.

Error Parameter	Value
Conic approximation	0.4 arcminute
Figure	0.6 arcminutes
Assembly	0.5 arcminutes
Scatter	0.1 arcminutes
TOTAL	0.9 arcminutes

Table 5: *HEFT* error budget.

ACKNOWLEDGMENTS

This work is Columbia Astrophysics Laboratory contribution number 642.

REFERENCES

1. K. Makishima, in Proc. Hinotori Symp. On Solar Flares (ed. Y. Tanaka et al.), 120, 1982.
2. W.W. Craig, et al., "Arcminute Resolution Gamma-ray Images of Cosmic Sources Taken with the Balloon-borne GRATIS Payload," BAAS, 93.04, 1997.
3. F.E. Christensen et al., "A graded d-spacing multilayer telescope for high-energy x-ray astronomy," Proc. SPIE, 1546, 160, 1992.
4. P.J. Serlemitsos and Y. Soong, "Foil X-ray Mirrors," LHEA/NASA preprint, 95-08, 1995.
5. N.J. Westergaard et al., "Status of the development of a thin foil throughput X-ray telescope for the Soviet Spectrum X-gamma mission," Opt. Eng., 29(6), 658, 1990.
6. R.C. Catura, E.G. Joki, D.T. Roethig and W.J. Brookover, "Lacquer polishing of x-ray optics," Applied Optics, 26(8), 1563, 1987.
7. K.D. Joensen, P. Gorenstein, O. Citterio, P. Hoghoj, I. Anderson and O. Schaerpf, "Hard X-ray Wolter-I telescope using broad-band multilayer coatings on replica substrates: Problems and Solutions, Proc. SPIE, 2515, 146, 1995.
8. "The High Throughput X-ray Spectroscopy (HTXS) Mission," An interim report to NASA by the HTXS Science Working Group, 1996 (unpublished).
9. Kahn, S.M et al "Reflection grating arrays for the Reflection Grating Spectrometer on board XMM", Proc. SPIE Vol. 2808, p. 450-462, 1996.
10. Mencik, J., "Strength and Fracture of Glass and Ceramics", Elsevier, Amsterdam, 1992.
11. J. Polny et al., "Assembly and alignment of the XSPECT Mirror Modules for the SODART X-ray telescope on the Spectrum Rontgen Gamma satellite," SPIE (this conference).